1 **Plant functional traits modulate the effects of soil acidification on above- and**

2 **belowground biomass**

3 Xue Feng [1], Ruzhen Wang [1,2], Tianpeng Li [1], Jiangping Cai [1], Heyong Liu [1,2], Hui Li [1],

4 Yong Jiang [1,2,*]

5 [1]Erguna Forest-Steppe Ecotone Ecosystem Research Station, Institute of Applied

6 Ecology, Chinese Academy of Sciences, Shenyang 110016, China

7 [2]College of Life Sciences, Hebei University, Baoding 071002, Hebei, China

9 * Correspondence: Yong Jiang (jiangyong@iae.ac.cn).

Abstract

Atmospheric sulfur (S) deposition has been extensively recognized as a major driving force of soil acidification. However, little is known on how soil acidification influences above- and belowground biomass via altering leaf and root traits.

A 3-year elemental S addition were conducted to simulate soil acidification in a meadow. Grass (*Leymus chinensis*) and sedge (*Carex duriuscula*) species were chosen to demonstrate the linkage between plant traits and biomass.

Sulfur addition led to soil acidification and nutrient imbalance. For *L. chinensis*, soil acidification decreased specific leaf area but increased leaf dry matter content showing a conservative strategy and thus suppression of aboveground instead of belowground biomass. For *C duriuscula*, soil acidification increased plant height and root nutrients (N, P, S, and Mn) for competing resources by investing more on above- and belowground biomass, *i.e.*, an acquisitive strategy. An overall reduction in community aboveground biomass by 3-33% resulted from the increased soil acidity. While the community root biomass increased by 11-22% as upregulated by higher soil nutrient availability.

Our results provide new insights that plant above- and belowground biomass is conditioned by S-invoked acidification and their linkages with plant traits contributed to a deeper understanding of plant-soil feedback.

Keywords: sulfur addition, soil acidification, meadow grassland, functional traits, plant biomass

1 Introduction

Acid deposition as a consequence of anthropogenic activities will have important impacts on terrestrial biodiversity and ecosystem functions and services (Tian and Niu, 2015; Clark et al., 2019; Yang et al., 2021). Atmospheric sulfur (S) deposition is one of the main causations of soil acidification, and its contribution is equal to or exceeds that of nitrogen (N) deposition in Asia (Duan et al., 2016; Zhang et al., 2022). Despite large decrease in average S deposition across China over the past decades, it is still very serious in Northeast China and Inner Mongolia (Yu et al., 2017). The northern grasslands of China as an integral part of the Eurasian grassland have experienced severe soil acidification with a significant decline in mean soil pH from 7.84 to 7.21 during 1980s- 2000s, while S deposition can undoubtedly accelerate this process (Yang et al., 2012). Therefore, soil acidification has become a major global concern, not only leading to soil nutrient losses but also decreasing the productivity of terrestrial ecosystems (Chen et al., 2013a; Tibbett et al., 2019; Duddigan et al., 2021).

In natural ecosystems, sulfur is an essential nutrient in forming plant proteins because it is a constituent of certain amino acids, but S limitation rarely occurs (Vitousek and Howarth, 1991; Garrison et al., 2000). Shifts in plant species and community associated with S deposition were mainly a consequence of soil acidification rather than a S-fertilization effect (Clark et al., 2019). This is because soil pH is a primary regulator of nutrient availability that plant growth and species co-existence rely on (Bolan et al., 2003; Tibbett et al., 2019). For instance, soil acidification inhibits nitrification (Kemmitt et al., 2005), but promotes the release of soil available phosphorus (P), micronutrients and the leaching of soil base cations (Jaggi et al., 2005; Chen et al., 2015; Feng et al., 2019). Evidence from contrived S addition experimentation has shown that aboveground biomass (AGB) decreased with soil acidification, whereas sedges with high acid tolerance revealed the opposite pattern in a subalpine grassland (Leifeld et al., 2013). The acidification-mediated decrease in soil cation concentrations (such as Ca^{2+} and NO_3^-) could increase the relative abundance of acid-tolerant and oligotrophic species (van Dobben and de Vries, 2010; Clark et al.,

62 2019) as a result of decreasing abundance of other species (Jung et al., 2018).

63 Additionally, soil Mn toxicity caused by soil acidification in calcareous grassland

64 asymmetrically curbed aboveground biomass of different species and functional groups

65 through suppression of photosynthesis (Tian et al., 2016).

66   A global meta-analysis with most data from forest ecosystems found negative

67 acidification effect on root biomass under sulfuric acid addition (Meng et al., 2019).

68 This was because forest soils with low initial pH (pH < 5) generally experienced greater

69 Al^{3+} and Fe^{3+} but less base cations, thus inhibiting root growth (Li et al., 2018).

70 Different from findings in forests, belowground biomass increased with soil

71 acidification in typical and alpine grasslands which was mainly due to the

72 compensatory growth concomitant with graminoids dominating over forbs (Chen et al.,

73 2015; Wang et al., 2020). Possibly, perennial rhizome grasses and sedges have higher

74 ionic tolerance (such as H^+, Al^{3+}, NH_4^+, and SO_4^{2-}) than perennial bunchgrasses and

75 forbs, which allowed for the maintenance of high community biomass under soil

76 acidification (Chen et al., 2015; Cliquet and Lemauviel-Lavenant, 2019; Wang et al.,

77 2020). Therefore, shifts in grassland community are mainly regulated by soil nutrient

78 fluctuations as induced by soil acidification that eventually affect above- and

79 belowground biomass (Mitchell et al., 2018; Wang et al., 2020).

80   Functional traits substantially influence plant survival, growth and reproduction via

81 closely associating with plant capability of resource acquisition (Violle et al., 2007).

82 Coping with environmental stresses to persist and reproduce, plants rely on a

83 combination of different functional traits ranging from conservative to acquisitive

84 strategies of resource acquisition (De Battisti et al., 2020). For example, some species

85 upregulate tissue nutrients as a fast resource acquisitive strategy when soil

86 environmental conditions become challenging (Mueller et al., 2012). On the opposite,

87 some plant species under environmental stresses tend to be more nutrient-conservative

88 by developing long-lasting leaves generally with a low specific leaf area (SLA) but a

89 high leaf dry matter content (LDMC) (Kandlikar et al., 2022). Grass species may also

90 increase root length to avoid acid and Al^{3+} stresses (Göransson et al., 2011). In general,

91 species with acquisitive strategy accumulate greater biomass in a rapid way, but species

92 with conservative strategy slow down biomass growth to elongate their life span (Reich,

93 2014; Hao et al., 2020).

94   Due to difficulties in measuring grassland root traits in situ, our understanding is

95 very limited in terms of using root trait strategy to explain the response of belowground

96 processes to soil acidification. Some plants can cope with nutrient deficiency in acidic

97 soils via modifications to their root morphologies and in their nutrient uptakes and

98 metabolisms (Hammond et al., 2004). Plants growing in resource-poor soils tend to

99 have lower specific root length (SRL) and lower root nutrient concentrations for the

100 conservation of resources (Delpiano et al., 2020). A pot experiment found that root

101 length of perennial grasses decreased with soil acidification, demonstrating the

102 constraint of root development in stressful circumstances (Haling et al., 2010). But in

103 natural ecosystems, grasses develop densely branched root systems with higher nutrient

104 use efficiency are more stress-tolerant to nutrient deficiency to maintain nutrient

105 balance and growth (Tian et al., 2022). Additionally, aboveground and belowground

106 biomass might also strongly and complicatedly be influenced by specific functional

107 traits (Clark et al., 2019; Wang et al., 2020), soil nutrient availability, and nutrient

108 contents and interactions in leaves and roots under soil acidification (Geng et al., 2014;

109 Rabêlo et al., 2018; Tian et al., 2021). Overall, it still remains elusive for how functional

110 traits in both above- and belowground components of different species respond to soil

111 acidification and their linkages with biomass.

112   To understand how soil acidification influences plant traits, biomass and their

113 relationships, we conducted a S addition experiment that included eight rates (from 0

114 to 50 g S m^{-2} yr^{-1}) to simulate soil acidification in a semiarid grassland. We assessed the

115 role of plant above- and belowground traits and soil abiotic variables in driving the

116 grassland biomass of two dominate species (*Leymus chinensis* and *Carex duriuscula*)

117 under soil acidification. Specifically, we also aimed to quantify how these relationships

118 were modified by changes in soil conditions and related trait response strategy. The

119 perennial rhizome grass, a taller *L. chinensis* is widely distributed in arid and semi-arid

120 areas of northern China. This species occupies the top layers of the studied grassland

121 communities, likely giving it an advantage in resource acquisition, especially in terms

122 of light. Additionally, grasses generally exhibit flexibility in absorbing various soil N

123 forms, thereby expanding their ecological niche (Grassein et al., 2015). The perennial

124 rhizomatous sedge, a shorter subordinate species *C. duriuscula*, indicator plant for soil

125 degradation, possesses cluster root, tends to consume more photosynthetic products to

126 acquire nutrients (Zhang et al., 2021). Moreover, both species exhibit distinct

127 rhizosheaths that enable them to tightly adhere to the soil and show compensatory

128 growth in response to environmental disturbance (Tian et al., 2022). We addressed the

129 following questions: (i) how do soil properties (*i.e.* soil pH, Ca^{2+}, Al^{3+}, available N,

130 available P), above- and belowground plant traits (*i.e.* morphological and nutrient traits)

131 and biomass respond to different rates of S addition in the meadow grassland? (ii) What

132 are the key traits that correlate with the biomass responses of two species to soil

133 acidification? We hypothesize that soil acidification caused by S addition would lead to

134 a nutrient imbalance in grassland soil. Grass *L. chinensis* may respond to soil

135 acidification by adapting its aboveground light acquisition traits to maintain plant

136 biomass. However, in acidified soil, sedge *C. duriuscula* may employ the increased

137 tissue nutrient concentrations as a strategy to improve its acid resistance, which

138 subsequently leads to compensatory root growth (Fig. S1).

139 **2 Materials and methods**

140 **2.1 Experimental site and design**

141 This study was conducted at the Erguna Forest-Steppe Ecotone Research Station (50°

142 10′ N, 119° 23′ E) of Chinese Academy of Sciences in Inner Mongolia, China. The area

143 belongs to a transitional climate zone between mid-temperate to cold-temperate climate

144 with mean annual temperature and precipitation of -2.45 °C and 363 mm, respectively

145 (Feng et al., 2019). Soil in the experimental site is classified as a Haplic Chernozem

146 according to the Food and Agricultural Organization of the United Nations

147 classification and composed of 37 ± 0.9% sand, 40 ± 1.0% silt and 24 ± 0.8% clay.

148 Vegetation in this area is a meadow steppe community including common plant species

149 of *Leymus chinensis*, *Stipa baicalensis*, *Cleistogenes squarrosa*, *Carex duriuscula*,

150 *Pulsatilla turczaninovii*, and *Cymbaria dahurica*.

151   The experimental field was a natural steppe, which had been mown annually for

152   forage harvest until 2013, and fenced to exclude livestock grazing since then. A field

153   elemental S addition experiment was established in 2017 to simulate soil acidification

154   caused by atmospheric S deposition in a homogeneous and flat field containing

155   naturally assembled communities. The vegetation in the experimental plots is composed

156   of the dominant species (relative abundance >40 %) *Leymus chinensis*, subordinate

157   species (relative abundance between 1 % and 30 %), including *Stipa baicalensis, Carex*

158   *duriuscula, Cleistogenes squarrosa, Achnatherum sibiricum, Cymbaria dahurica,*

159   *Pulsatilla turczaninovii, Thermopsis lanceolala* and *Achnatherum sibiricum*. A

160   randomized block design was exploited included eight levels of S addition (0, 1, 2, 5,

161   10, 15, 20, and 50 g S m^{-2} yr^{-1}), and each treatment had five replicates (Fig. S2). The

162   low dose S applications in our study was to imitate the current atmospheric SO_4^{2-}

163   deposition level (2 - 4 g S m^{-2} yr^{-1}) in the northeast of China (Yu et al., 2017). Each plot

164   (6 m × 6 m) was surrounded by 2-m wide buffer strips. Purified sulfur fertilizer

165   (elemental S > 99%) was mixed with 200 g soil collected from the untreated site nearby

166   and applied by hand spreading annually in late May since 2017. Sulfur powder in soil

167   can be oxidized by soil microorganisms to form H^+ and SO_4^{2-} which can simulate soil

168   acidification well (Duddigan et al., 2021). In present study, we collected plant and soil

169   samples from 25 plots (five replicates) supplemented with five levels of S (0, 5, 10, 20,

170   and 50 g S $m^{-2}yr^{-1}$).

171   2.2 Plant and soil sampling

172   In early August 2019, aboveground net primary productivity (ANPP) of plant

173   communities was collected from peak aboveground plant biomass because all

174   aboveground plant tissues would die during the winter. All living tissues were clipped

175   within a randomly selected 1 m × 1 m quadrat in each plot, sorted by species and oven-

176   dried at 65 °C for 48 h to measure peak species biomass and ANPP. The dried plant

177   samples were prepared to measure leaf nutrients.

178   We measured three aboveground morphological traits for two dominant species

179   *Leymus chinensis* (*L. chinensis*) and *Carex duriuscula* (*C. duriuscula*). Ten plant

180   individuals with complete shoot were randomly selected in each plot for each species.

181   These plant individuals were measured for maximum natural height and then clipped at

182   the ground level. All the samples immediately were placed in a portable refrigerator

183   and then detached to measure leaf area in laboratory. To guarantee water saturation of

184   the leaves, the sampled leaves were immersed in purified water and rehydrated for a

185   minimum period of 6 hours. Then the water-saturated leaves were carefully wiped off

186   the surface water with filter paper and weighed. The leaf area was scanned using a

187   scanner (Eption Perfection V39, Seiko Epson Corporation, Japan) and then dried at

188   60 °C for 72 h to weigh for dry mass. Specific leaf area (SLA, $cm^2\ g^{-1}$) was calculated

189   as the ratio of leaf area to dry mass. Leaf dry matter content was calculated as the ratio

190   of dry mass to saturated mass (LDMC, $g\ g^{-1}$).

191   Plant roots were sampled using the soil block method in late August 2019.

192   Specifically, a 30 cm (length) × 30 cm (width) × 30 cm (depth) soil block was collected

193   using a steel plate and a shovel from each plot, resulting in a total of 25 soil blocks.

194   Each harvested soil block was immediately transported to the processing area and then

195   the soil blocks were gently loosened by hands to separate roots from soils. All separated

196   plant roots were carefully washed to remove the adhering soil and stored in iceboxes to

197   the laboratory. Before determining root morphological and chemical traits, all root

198   samples were frozen at -20 °C. At least 10 intact individual plants of *L. chinensis* and

199   *C. duriuscula* in each plot were used for determining root nutrient traits (root [N], [P],

200   [S], [Ca], [Fe], and [Mn]) and root morphological traits. Total root length, surface area

201   and volume were determined using the scanned images by the software of WinRHIZO

202   (Regent Instruments Inc., Quebec City, QC, Canada). Specific root length (SRL, $m\ g^{-1}$)

203   was calculated as total root length divided by its dry mass. Specific root surface area

204   (SRA, $cm^2\ g^{-1}$) was defined as total surface area divided by its dry mass. Root tissue

205   density (RTD, $g\ cm^{-3}$) was obtained as the ratio of root dry mass to its volume. All of

206   the above samples were dried at 65 °C to constant mass for determining root biomass

207   at species and community level. Root and leaf N concentrations were determined using

208   an elemental analyzer (Vario EL III, Elementar, Hanau, Germany). Both root and leaf

209   P, S, Ca, Fe and Mn concentrations were digested with 8 mL HNO_3 + 4 mL $HClO_4$ and

210 then determined by inductively coupled plasma optical emission spectrometry (5100

211 ICP-OES; Perkin Elmer, America).

212   Fresh soil sampling (0 - 10 cm depth) was performed using a soil auger (5 cm inner

213 diameter). For each plot, three cores were combined into one homogeneous sample.

214 After removing the visible plant detritus and rock, we sieved the fresh soils through a

215 2-mm screen and divided each soil sample into two subsamples. Then a 10 g of fresh

216 soil was immediately extracted with 2 mol L^{-1} KCl solution. The extracted solution was

217 analyzed for nitrate (NO_3^-) and ammonium (NH_4^+) concentrations using an

218 autoAnalyser III continuous Flow Analyzer (Bran and Luebbe, Norderstedt, Germany).

219 The other subsample was air-dried for physicochemical properties determination. Soil

220 pH was determined in 2.5: 1 (v/w) water/soil ratio with a digital pH meter (Precision

221 and Scientific Instrument Co. Ltd., Shanghai, China). Soil available P concentration

222 was extracted with 0.5 mol L^{-1} NaHCO$_3$ solution and soil available S concentration was

223 extracted with 0.1 mol L^{-1} Ca(H$_2$PO$_4$)$_2$ (Tabatabai and Bremner, 1972) following

224 absorbance measurement on a UV-VIS spectrophotometer (UV-1700, Shimadzu, Japan)

225 at 880 nm and 440 nm, respectively. Soil exchangeable aluminum (Al^{3+}) concentration

226 was measured using titration by 0.25 M NaOH to pH 7.0 after extraction with 1 M KCl

227 solution from air-dried soil samples. Soil exchangeable calcium (Ca^{2+}) was extracted

228 by 1 M NH$_4$OAc (pH = 7.0) at a 1:10 ratio (w/v) for 30 min. Diethylene triamine

229 pentaacetic acid (DTPA)-Fe and Mn were extracted from 10 g of air-dried soil sample

230 with 20 ml of 0.005 M diethylenetriamine pentaacetic acid (DTPA), 0.01 M CaCl$_2$, and

231 0.1 M triethanolamine (TEA) at pH 7.3 and determined using an atomic absorption

232 spectrophotometer (AAS, Shimadzu, Japan) (Feng et al., 2019; Li et al., 2021).

233 **2.3 Statistical analyses**

234 The effects of S addition on soil properties, plant traits and biomass were analyzed using

235 one-way analysis of variance (ANOVA) with Duncan test. Pearson's correlation

236 analysis was used to explore the relationship between plant traits, plant biomass and

237 soil abiotic variables across the S-addition levels. All these statistical analyses were

238 performed using SPSS16.0 (SPSS Inc., Chicago, USA) with significance accepted at *p*

239   < 0.05.

240   We used structural equation modelling (SEM) to analyze the indirect effects of S

241   addition meditating grassland plant aboveground and root biomass from the perspective

242   of plant traits and soil factors. Prior to SEM analysis, the number of variables were

243   reduced by conducting principal component analysis (PCA) on soil variables (pH,

244   NH_4^+-N, NO_3^--N, available P, available S, exchangeable cations Ca^{2+} and Al^{3+}, DTPA-

245   Fe and DTPA-Mn), aboveground morphological traits (Height, SLA, LDMC), leaf

246   nutrient traits (Ca, Fe, Mn), root morphological traits (SRL, SRA, RTD) and root

247   nutrient traits (N, P, S, Ca, Fe, Mn) of the two species. We then used the first principal

248   components (PC1) for the subsequent SEM analysis to represent soil acidification (PC1

249   explained 94.8% of the variation), soil nutrients (PC1 explained 62.3% of the variation),

250   root nutrient traits in *C. duriuscula* (PC1 explained 45.7% of the variation),

251   aboveground morphological traits in *L. chinensis* (PC1 explained 54.7% of the variation)

252   (Table S1). A conceptual model of hypothetical relationships was constructed (Fig. S1),

253   assuming that S addition would directly impact soil physicochemical properties, and

254   indirectly influence aboveground and belowground biomass through altering soil pH,

255   soil nutrient availability and plant traits. The SEM analyses were performed using

256   AMOS 24.0 (Amos Development Co., Maine, USA) and the PCA analyses were

257   performed using the vegan package in R 4.2.2.

258

3 Results

3.1 Effects of S addition on soil properties

261   Sulfur addition significantly decreased soil pH from 6.95 to 5.19, but increased soil

262   exchangeable Al concentration only in the highest S-addition level of 50 g S m^{-2} yr^{-1}

263   (Table 1). Similarly, S addition increased soil ammonium concentration but decreased

264   nitrate concentration in the highest S addition treatment compared to the control (Table

265   1). Soil available P, available S, DTPA-Fe and DTPA-Mn concentration increased with

266   increasing S addition rate, while soil exchangeable Ca concentration decreased (Table

267   1).

3.2 Effects of S addition on above- and belowground biomass

In the third year, S addition suppressed aboveground biomass of plant community (Fig. 1). Aboveground biomass of the two dominant species showed contrasting responses to S addition, with an increase for *C. duriuscula* but a decrease for *L. chinensis* (Fig. 1). Moreover, S addition significantly increased belowground biomass of plant community owing to the increase in *C. duriuscula*, while it had no impact on the belowground biomass of *L. chinensis* (Fig. 1).

3.3 Effects of S addition on above- and belowground traits of *L. chinensis* and *C. duriuscula*

For the morphological traits, S addition enhanced plant height of *C. duriuscula*, but had no impact on *L. chinensis* (Fig. 2a). Sulfur addition significantly decreased SLA and increased LDMC of *L. chinensis*, whereas it had no effect on that of *C. duriuscula* (Fig. 2b and c). For the belowground tissues, S treatment increased SRL in two species, and only decreased SRA of *C. duriuscula* (Fig. 2d and e). However, RTD showed no significant change for the two species (Fig. 2f).

For the nutrient traits, S addition had no impact on leaf [N], [P], and [Ca], and increased leaf [S] and [Mn] of the two species, while decreased leaf [Fe] of *C. duriuscula* but increased leaf [Fe] of *L. chinensis* (Fig. 3). An increase in root [N], root [P], root [S] of *C. duriuscula* was found under S addition, but not for *L. chinensis* (Fig. 3h, i and j). Sulfur addition decreased root [Ca] of *C. duriuscula*, but had no impact on *L. chinensis* (Fig. 3k). Root [Fe] showed similar patterns with leaf [Fe] with a decrease in *C. duriuscula* and an increase in *L. chinensis* (Fig. 3l). Root [Mn] of species were enhanced by S addition (Fig. 3m).

3.4 Correlations and pathways of S-induced soil acidification effects on plant traits and biomass

According to correlation analysis (Figs. S3 and S4), the aboveground morphological traits, leaf and the root nutrient traits showed species-specific responses. This was mainly due to the increase in soil acidity, Al^{3+} toxicity and nutrient imbalance (*i.e.*, the

296 deficient or excessive of certain nutrients in the soil) induced by S addition, which fitted

297 the structural equation modelling (SEM) well (χ^2 =51.83, P = 0.10, df = 40, AIC =

298 103.83, n = 25) (Fig. 4). The indirect positive effect of S addition on community

299 belowground biomass was mainly implemented through decreasing soil pH together

300 with the imbalance of soil available nutrients, altering the leaf and root nutrient traits,

301 and the belowground biomass and of *C. duriuscula*, which accounted for 69% of the

302 variation in community belowground biomass (Fig. 4). The indirect negative effect of

303 S addition on community aboveground biomass was mainly achieved through soil

304 acidification, the aboveground morphological traits and aboveground biomass of *L.*

305 *chinensis*, which accounted for 59% of the variation in community aboveground

306 biomass (Fig. 4).

307 **4. Discussion**

308 **4.1 Species-specific trait responses to S addition**

309 Trait response patterns was different between *L. chinensis* and *C. duriuscula* under S

310 addition. Specifically, nutrient traits of *L. chinensis* were less plastic, as evidenced by

311 unchanged concentrations of N, P, S, and Ca, comparing with *C. duriuscula*. Indeed, *L.*

312 *chinensis* was suggested to be a highly homoeostatic species with greater stability in

313 elemental composition in a temperate steppe (Yu et al., 2010). Higher macroelement

314 homeostasis helps plant maintain function and productivity stability to resist changes

315 in soil environment (Yu et al., 2010; Feng et al., 2019).

316   It was interesting to note that both leaf and root [Fe] in *L. chinensis* increased with

317 S addition and were not associated with soil available [Fe] (Figs. 3 and S3). Iron uptake

318 and assimilation had been shown to be dependent on sulfate availability (Zuchi et al.,

319 2012). Previous research demonstrated close relationships between Fe and S nutrition,

320 suggesting common regulatory mechanisms for the homeostasis of the two elements

321 (Forieri et al., 2013). For grasses, S addition could enhance assimilation of plant S and

322 subsequently incorporated into methionine in order to accelerate the secretion of

323 phytosiderophore (Zuchi et al., 2012; Courbet et al., 2019). However, Fe absorption of

324 *C. duriuscula* was inhibited by soil acidification which was consistent with Fe (III)-

325 reduction-based mechanism (Tian et al., 2016). Namely, acquisition of Fe by non-

326 graminaceous monocotyledonous species was mediated by the reduction of Fe^{3+} to Fe^{2+}

327 catalyzed by the ferric chelate reductase in root cells, and Fe^{2+} absorption can be further

328 curbed by the competition with Mn^{2+} for the same metal transporter (Curie and Briat,

329 2003; Pittman, 2005). Acidification-induced higher soil DTPA-Mn concentration in the

330 calcareous soil contributed to Mn accumulation in plant tissues of the two species (Figs.

331 3 and 5). Sulfur addition increased tissue [Mn] greater in *C. duriuscula* than in *L.*

332 *chinensis*.

333   *L. chinensis* decreased SLA and increased LDMC to reduce the loss of water and

334 nutrients, which showed conservative resource-uptake strategy under soil acidification

335 stress. The variations in SLA and LDMC of *L. chinensis* were significantly correlated

336 with soil exchangeable Al, implying that conservative traits might also link with Al-

337 resistant strategy of species (Poozesh et al., 2007). As soil pH decreased, soil nitrate

338 was reduced and positively correlated with SLA but negatively with LDMC of *L.*

339 *chinensis* (Table 1 and Fig. S3). Soil nitrification had been shown to be positively

340 related to leaf traits (such as leaf [N] and SLA) (Laughlin et al., 2011). This suggested

341 that the decrease of soil nitrate under soil acidification could be an important driver of

342 plant trait variation. For *L. chinensis*, belowground traits were insensitive to S addition

343 as compared with *C. duriuscula*. One possible explanation for this insensitivity might

344 be that deep-rooted species were much more resistant to changing soil environment

345 than the shallow-rooted species (such as sedge *C. duriuscula*) (Zhang et al., 2019). We

346 found both species invested more in enhancing SRL under soil acidification, which was

347 in agreement with Göransson et al. (2011) that grass species increased root length to

348 avoid acid stress. These results indicated that variation of root morphological traits has

349 the potential to mitigate the negative effects of soil acidity and should be considered as

350 part of stress-avoidance or tolerance strategies (Thomaes et al., 2013).

351 **4.2 Species-specific and community biomass responses to S addition**

352 To clarify the underlying mechanisms, we explored the important role of morphological

353 and nutrient traits in mediating aboveground and belowground biomass changes under

354 S addition. We found that aboveground and root traits of two species exhibited

355 contrasting adaptive strategies in acquiring aboveground and belowground resources

356 which were associated with their biomass (Figs. 4 and 5). Importantly, SEM showed

357 that the decrease in aboveground biomass of *L. chinensis* was related to the increased

358 soil acidification and the conservative responses in aboveground morphological traits

359 under S addition (Figs. 4 and 5). *L. chinensis* seemed to be a nitrophilic and resource-

360 acquisitive species under N-rich environment (Feng et al., 2019; Yang et al., 2019), but

361 it was at a disadvantage under S-induced soil acidification. For example, we found SLA

362 and LDMC in *L. chinensis* were positively correlated with the aboveground biomass of

363 both *L. chinensis* and plant community (Fig. S3). Soil acidification resulted in enhanced

364 toxic effects of proton and exchangeable Al (Roem and Berndse, 2000). From

365 environmental stress hypothesis perspective, the species could employ different

366 strategies to mitigate such environmental stress which associated with trait responses

367 (Encinas-Valero et al., 2022). Usually, SLA and LDMC were prominent indicators of

368 plant strategy with respect to productivity as related to environmental stress and

369 disturbance regimes. Stress tolerant species normally had lower growth rates,

370 photosynthetic rates, and SLA but higher LDMC (Pérez-Harguindeguy et al., 2013).

371 Sulfur addition induced acidity stress for plants, leading to reduced SLA accompanied

372 with lower photosynthesis and decreased plant aboveground productivity. Damages in

373 photosynthetic function accompanied by oxidative stress were found in woody tree

374 species under the threat of acid rain (Chen et al., 2013b), it is still less understanding to

375 physiological and biochemical responses of different functional groups to soil

376 acidification in grassland ecosystems. The future researches about plant photosynthetic

377 and antioxidant responses by soil acidification are critically needed to test.

378   We found that plant community aboveground biomass exhibited a tendency to

379 decline from 22% to 11% under soil acidification, although the overall effect was rather

380 weak between pH 6.7 and pH 5.19 (Fig. 1, Table 1). Notably, *L. chinensis* played a

381 dominant role in aboveground productivity which was consistent with the finding that

382 grasses occupied a mean coverage of around 60% in acid grassland and Heathland

383 (Tibbett et al., 2019). Therefore, the decreasing aboveground biomass of *L. chinensis*

384 was one reason for the decline of community aboveground productivity (Fig. 4).

385 Another explanation for the decline of aboveground biomass may be competitive

386 exclusion of bunchgrasses and forbs under soil acidification (Stevens et al., 2010; Chen

387 et al., 2015). Together, our study contributes to a deeper understanding that leaf

388 morphological traits of dominant species play a crucial role in regulating grassland

389 productivity in response to soil acidification.

390 In contrast, belowground biomass of *C. duriuscula* and plant community both

391 significantly increased (ranging from 19 to 52%) with soil acidification (Fig. 1). Sedge

392 (*C. duriuscula*) was more tolerant than perennial rhizome grass (*L. chinensis*) under

393 soil acidification. This was partly supported by similar results obtained in alpine and

394 typical steppe grassland ecosystems (Chen et al., 2015; Wang et al., 2020). Previous

395 studies suggested that the sedge had a greater competitive advantage in nutrient-poor

396 environments than other functional groups (Gusewell, 2004). An increase in root

397 biomass under soil acidification suggested that sedge invested more resources in

398 nutrient acquisition. SEM provided further evidence that for *C. duriuscula*, the higher

399 nutrient demand (such as root [N], [P], [S], [Mn]) was matched by high root biomass

400 investment under S treatment (Fig. 4). The increased root biomass of *C. duriuscula*

401 promoted the increased belowground biomass of plant community which could be

402 related to the shifts in soil available nutrients under S addition. Our present study

403 provided direct evidence that *C. duriuscula* was considered to be a high nutrient-

404 requiring species and thereby its biomass growth increased with soil acidification stress

405 (Figs. 4 and 5). Our short-term findings suggest that the sedge play an important role in

406 preventing the decline of grassland productivity in acidified soils, reflecting transient

407 dynamics. Consistent with results from a long-term acidification experiment (Tibbett et

408 al., 2019), compensatory growth of acid-tolerant species is probably key to maintain

409 grassland productivity over the long term, particularly for ecosystems that experience

410 acidification by chronic N and S deposition.

411 For grassland ecosystems, most of the carbon is allocated belowground (Bontti et

412 al., 2009). Accumulation of roots may benefit competition for nutrient and water

413 resources in a short-term (Wang et al., 2020). In the long-term, however, asymmetric

light competitive advantage of larger individuals (*L. chinensis*) rather than the competition of soil resources (DeMalach and Kadmon, 2017), will make a decisive effect on community productivity and diversity under soil acidification. Contrary to previous findings by Wang et al. (2020), who reported that diameter of 3rd-order roots contributed to the increase of community belowground biomass under soil acidification in an alpine grassland. Our study provided a novel insight that leaf and root nutrients as a whole jointly mediated community belowground biomass with soil acidification induced by S addition.

5 Conclusion

Our results highlighted that aboveground and root traits played important roles in mediating grassland plant competition for environment resources under soil acidification. Sulfur addition acidified soils, and lead to nutrient imbalance (higher ammonium, available P, Fe, Mn and exchangeable Al^{3+}, but lower nitrate and exchangeable Ca^{2+}). The dominant species *L. chinensis* showed conservative strategy, with decreased SLA and increased LDMC in response to S addition. Moreover, conservative traits were linked with stable root biomass but lower aboveground biomass as a direct impact from soil acidification. Conversely, *C. duriuscula* displayed acquisitive strategy, with increased shoot height and root traits ([N], [P], [S], [Mn], SRL) promoting both aboveground and root biomass under S addition, as mediated via altered soil acidity and nutrient availability. Such divergent and species-specific responses was strongly driven by soil environmental conditions which resulted in inconsistent responses of grassland community aboveground and belowground biomass to S addition. As continuous S deposition causes widespread acidification and soil functional degradation problems across the world, our results implied the important roles of both aboveground and root traits in regulating species and community biomass under soil acidification.

Author contributions. All authors contributed to the design of the study. TL and HL conducted the experimental work and the data analysis. XF wrote the manuscript with

443   RW, JC and YJ.

444

445   *Competing interests.* None of the authors have a conflict of interest.

446

447   *Acknowledgements.* We would like to acknowledge the support from Youth

448   Innovation Promotion Association of Chinese Academy of Sciences.

449

450   *Financial support.* This research was supported by the National Natural Science

451   Foundation of China (32271677, 32071563, 32222056 and 32271655), the Strategic

452   Priority Research Program of the Chinese Academy of Sciences (XDA23080400), and

453   the Doctoral Science Foundation of Liaoning Province (2021-BS-015).

454

455

456   *Data availability.* Data will be made available on request from the corresponding

457   author.

458

References

460   Bolan, N. S., Adriano, D. C., and Curtin, D.: Soil acidification and liming interactions

461   with nutrient and heavy metal transformation and bioavailability, Adv. Agron.,

462   78, 5-272, https://doi.org/10.1016/S0065-2113(02)78006-1, 2003.

463   Bontti, E. E., Decant, J. P., Munson, S. M., Gathany, M. A., Przeszlowska, A., Haddix,

464   M. L., Owens, S., Burke, I. C., Parton, W. J., and Harmon, M. E.: Litter

465   decomposition in grasslands of central North America (US Great Plains), Global

466   Chang Biol., 15, 1356-1363. https://doi.org/ 10.1111/j.1365-2486.2008.01815.x,

467   2009.

468   Chen, D., Lan, Z., Bai, X., Grace, J. B., and Bai, Y.: Evidence that acidification-

469   induced declines in plant diversity and productivity are mediated by changes in

470   below-ground communities and soil properties in a semi-arid steppe, J. Ecol.,

471   101, 1322-1334, https://doi.org/10.1111/1365-2745.12119, 2013a.

472 Chen, D., Wang, Y., Lan, Z., Li, J., Xing, W., Hu, S. and Bai, Y.: Biotic community

473   shifts explain the contrasting responses of microbial and root respiration to

474   experimental soil acidification, , 90, 139-147,

475   https://doi.org/10.1016/j.soilbio.2015.08.009, 2015.

476 Chen, J., Wang, W. H., Liu, T., Wu, F., and Zheng, H.: Photosynthetic and antioxidant

477   responses of *Liquidambar formosana* and *Schima superba* seedlings to sulfuric-

478   rich and nitric-rich simulated acid rain. Plant Physiol. Bioch., 64, 41-51,

479   https://doi.org/10.1016/j.plaphy.2012.12.012, 2013b.

480 Clark, C. M., Simkin, S. M., Allen, E. B., Bowman, W. D., Belnap, J., Brooks, M. L.,

481   Collins, S. L., Geiser, L. H., Gilliam, F, S., Jovan, F. S., Pardo, L. H., Schulz, B.

482   K., Stevens, C. J., Suding, K. N., Throop, H. L., and Waller, D. M.: Potential

483   vulnerability of 348 herbaceous species to atmospheric deposition of nitrogen

484   and sulfur in the United States, Nat. Plants, 5, 697-705, https://doi.org/10.1038/

485   s41477-019-0442-8, 2019.

486 Cliquet, J. B. and Lemauviel-Lavenant, S.: Grassland species are more efficient in

487   acquisition of S from the atmosphere when pedospheric S availability decreases,

488   Plant Soil, 435, 69-80, https://doi.org/10.1007/s11104-018-3872-6, 2019.

489 Courbet, G., Gallardo, K., Vigani, G., Brunel-Muguet, S., Trouverie, J., Salon, C., and

490   Ourry, A.: Disentangling the complexity and diversity of crosstalk between sulfur

491   and other mineral nutrients in cultivated plants, J. Exp. Bot., 70, 4183-4196,

492   https://doi.org/10.1093/jxb/erz214, 2019.

493 Curie, C. and Briat, J. F.: Iron transport and signaling in plants, Annu. Rev. Plant

494   Biol.*,* 54, 183-206, https://doi.org/10.1146/annurev.arplant.54.031902.135018,

495   2003.

496 De Battisti, D., Fowler, M. S., Jenkins, S. R., Skov, M. W., Bouma, T. J., Neyland, P.

497   J., and Griffin, J. N.: Multiple trait dimensions mediate stress gradient effects on

498   plant biomass allocation, with implications for coastal ecosystem services, J.

499   Ecol., 108, 1227-1240, https://doi.org/10.1111/1365-2745.13393, 2020.

500 Delpiano, C.A., Prieto, I., Loayza, A.P., Carvajal, D.E., and Squeo, F.A.: Different

501   responses of leaf and root traits to changes in soil nutrient availability do not

502   converge into a community-level plant economics spectrum. Plant Soil 450, 463-

503   478, https://doi.org/10.1007/s11104-020-04515-2, 2020.

504 DeMalach, N. and Kadmon, R.: Light competition explains diversity decline better

505   than niche dimensionality, Funct. Ecol., 31, 1834-1838, https://doi.org/10.1111/

506   1365-2435.12841, 2017.

507 Duan, L., Yu, Q., Zhang, Q., Wang, Z., Pan, Y., Larssen, T., Tang, J., and Mulder, J.:

508   Acid deposition in Asia: Emissions, deposition, and ecosystem effects,

509   Atmospheric Environ., 146, 55-69, http://doi.org/10.1016/j.atmosenv.2016.07.

510   018, 2016.

511 Duddigan, S., Fraser, T., Green, I., Diaz, A., Sizmur, T., and Tibbett, M.: Plant, soil

512   and faunal responses to a contrived pH gradient, Plant Soil, 462, 505-524,

513   https://doi. org/10.1007/s11104-021-04879-z, 2021.

514 Encinas-Valero, M., Esteban, R., Hereş, A. M., Vivas, M., Fakhet, D., Aranjuelo, I.,

515   Solla, A., Moreno, G., and Curiel Yuste, J.: Holm oak decline is determined by

516   shifts in fine root phenotypic plasticity in response to belowground stress, New

517   Phytol., 235, 2237-2251, https://doi.org/10.1111/nph.18182, 2022.

518 Feng, X., Wang, R., Yu, Q., Cao, Y., Zhang, Y., Yang, L., Dijkstra, F. A., and Jiang, Y.:

519   Decoupling of plant and soil metal nutrients as affected by nitrogen addition in a

520   meadow steppe, Plant Soil, 443, 337-351, https://doi.org/10.1007/s11104-019 -

521   04217-4, 2019.

522 Forieri, I., Wirtz, M., and Hell, R.: Toward new perspectives on the interaction of iron

523   and sulfur metabolism in plants, Front. Plant Sci., 4, 357, https://doi.org/10.3389

524   /fpls.2013.00357, 2013.

525 Garrison, M. T., Moore, J. A., Shaw, T. M., and Mika, P. G.: Foliar nutrient and tree

526   growth response of mixed-conifer stands to three fertilization treatments in

527   northeast Oregon and north central Washington, For. Ecol. Manag., 132, 183-

528   198, https://doi.org/10.1016/S0378-1127(99)00228-5, 2000.

529 Geng, Y., Wang, L., Jin, D., Liu, H., and He, J.: Alpine climate alters the relationships

530   between leaf and root morphological traits but not chemical traits, Oecologia,

531 175, 445-455, https://doi.org/10.1007/s00442-014-2919-5, 2014.

532 Göransson, P., Falkengren-Grerup, U., and Andersson, S.: *Deschampsia cespitosa* and

533  soil acidification: general and trait-specific responses to acid and aluminium

534  stress in a solution experiment, Nord. J. Bot., 29, 97-104, https://doi.org/10.1111

535  /j.1756-1051.2010.00793.x, 2011.

536 Grassein, F., Lemauviel- Lavenant, S., Lavorel, S., Bahn, M., Bardgett, R. D.,

537  Desclos- Theveniau, M., and Laîné, P.: Relationships between functional traits

538  and inorganic nitrogen acquisition among eight contrasting European grass

539  species. Ann. Bot., 115, 107-115, https://doi.org/10.1093/aob/mcu233, 2015.

540 Gusewell, S.: N: P ratios in terrestrial plants: Variation and functional significance.

541  New Phytol., 164, 243-266, https://doi.org/10.1111/j.1469-8137.2004.01192.x,

542  2004.

543 Haling, R. E., Richardson, A. E., Culvenor, R. A., Lambers, H., and Simpson, R. J.:

544  Root morphology, root-hair development and rhizosheath formation on perennial

545  grass seedlings is influenced by soil acidity, Plant Soil, 335, 457-468, https://

546  doi.org/10.1007/s11104-010-0433-z, 2010.

547 Hammond, J.P., Broadley, M. R., and White, P. J.: Genetic responses to phosphorus

548  deficiency. Ann. Bot., 94, 323-332, https://doi.org/10.1093/aob/mch156, 2004.

549 Hao, M., Messier, C., Geng, Y., Zhang, C., Zhao, X., and von Gadow, K.: Functional

550  traits influence biomass and productivity through multiple mechanisms in a

551  temperate secondary forest, Eur. J. For. Res., 139, 959-968, https://doi.org/10.

552  1007/s10342-020-01298-0, 2020.

553 Jaggi, R. C., Aulakh, M. S., and Sharma, R.: Impacts of elemental S applied under

554  various temperature and moisture regimes on pH and available P in acidic,

555  neutral and alkaline soils, Biol. Fert. Soils, 41, 52-58,

556  https://doi.org/10.1007/s00374 -004-0792-9, 2005.

557 Jung, K., Kwak, J. H, Gilliam, F. S., and Chang, S. X.: Simulated N and S deposition

558  affected soil chemistry and understory plant communities in a boreal forest in

559  western Canada. J. Plant Ecol., 11, 511-523, https://doi.org/10.1093/jpe/rtx030,

560  2018.

561   Kandlikar, G. S., Kleinhesselink, A. R., and Kraft, N. J.: Functional traits predict

562   species responses to environmental variation in a California grassland annual

563   plant community, J. Ecol., 110, 833-844, https://doi.org/10.1111/1365-

564   2745.13845, 2022.

565   Kemmitt, S. J., Wright, D., and Jones, D. L.: Soil acidification used as a management

566   strategy to reduce nitrate losses from agricultural land, Soil Biol. Biochem., 37,

567   867-875, https://doi.org/10.1016/j.soilbio.2004.10.001, 2005.

568   Laughlin, D.C.: Nitrification is linked to dominant leaf traits rather than functional

569   diversity, J. Ecol., 99, 1091-1099, https://doi.org/10.1111/j.1365-2745.2011.

570   01856.x, 2011.

571   Leifeld, J., Bassin, S., Conen, F., Hajdas, I., Egli, M., and Fuhrer, J.: Control of soil

572   pH on turnover of belowground organic matter in subalpine grassland,

573   Biogeochemistry, 112, 59-69, https://doi.org/10.1007/s10533-011-9689-5, 2013.

574   Li, T., Wang, R., Cai, J., Meng, Y., Wang, Z., Feng, X., Liu, H., Turco, R. F., and

575   Jiang, Y.: Enhanced carbon acquisition and use efficiency alleviate microbial

576   carbon relative to nitrogen limitation under soil acidification, Ecol. Process, 10,

577   1-13, https://doi.org/10.1186/s13717-021-00309-1, 2021.

578   Li, Y., Sun, J., Tian, D., Wang, J., Ha, D., Qu, Y., Jing, G., and Niu, S.: Soil acid

579   cations induced reduction in soil respiration under nitrogen enrichment and soil

580   acidification, Sci. Total Environ., 615, 1535-1546, http://doi.org/10.1016/j.

581   scitotenv.2017.09.131, 2018.

582   Meng, C., Tian, D., Zeng, H., Li, Z., Yi, C., and Niu, S.: Global soil acidification

583   impacts on belowground processes, Environ. Res. Lett., 14, 074003, https://

584   doi.org/10.1088/1748-9326/ab239c, 2019.

585   Mitchell, R. J., Hewison, R. L., Fielding, D. A., Fisher, J. M., Gilbert, D. J.,

586   Hurskainen, S., Pakeman, R.J., Potts, J. M., and Riach, D.: Decline in

587   atmospheric sulphur deposition and changes in climate are the major drivers of

588   long-term change in grassland plant communities in Scotland, Environ. Pollut.,

589   235, 956-964, https:// doi.org/10.1016/j.envpol.2017.12.086, 2018.

590   Mueller, K. E., Eissenstat, D. M., Hobbie, S. E., Oleksyn, J., Jagodzinski, A. M.,

591   Reich, P. B., Chadwick, O. A., and Chorover. J.: Tree species effects on coupled

592   cycles of carbon, nitrogen, and acidity in mineral soils at a common garden

593   experiment, Biogeochemistry, 111, 601-614, https://doi.org/10.1007/s10533-011-

594   9695-7, 2012.

595   Pérez-Harguindeguy, N., Diaz, S., Garnier, E., Lavorel, S., Poorter, H., Jaureguiberry,

596   P., Bret-Harte, M. S, Cornwell, W. K., Craine, J. M., Gurvich, D. E., Urcelay, C.,

597   Veneklaas, E. J., Reich, P. B., Poorter, L., Wright, I. J., Ray, P., Enrico, L.,

598   Pausas, J. G., de Vos, A. C., Buchmann, N., Funes, G., Quetier, F., Hodgson, J.

599   G., Thompson, K., Morgan, H. D., ter Steege, H., van der Heijden, M. G. A.,

600   Sack, L., Blonder, B., Poschlod, P., Vaieretti, M. V., Conti, G., Staver, A. C.,

601   Aquino, S., and Cornelissen, J. H. C.: New handbook for standardised

602   measurement of plant functional traits worldwide, Aust. Bot., 61, 167-234,

603   http://doi.org/10.1071/BT 12225, 2013.

604   Pittman, J. K.: Managing the manganese: molecular mechanisms of manganese

605   transport and homeostasis, New Phytol., 167, 733-742, http://doi.org/10.1111/

606   j.1469-8137.2005.01453.x, 2005.

607   Poozesh, V., Cruz, P., Choler, P., and Bertoni, G., Relationship between the Al

608   resistance of grasses and their adaptation to an infertile habitat, Ann. Bot., 99,

609   947-954, https://doi.org/10.1093/aob/mcm046, 2007.

610   Rabêlo, F. H. S., Lux, A., Rossi, M. L., Martinelli, A. P., Cuypers, A., and Lavres, J.

611   Adequate S supply reduces the damage of high Cd exposure in roots and

612   increases N, S and Mn uptake by Massai grass grown in hydroponics, Environ.

613   Exp. Bot., 148, 35-46, https://doi.org/10.1016/j.envexpbot.2018.01.005, 2018.

614   Reich, P. B.: The world-wide 'fast-slow' plant economics spectrum: a traits manifesto,

615   J. Ecol., 102, 275-301, https://doi.org/10.1111/1365-2745.12211, 2014.

616   Roem, W. J. and Berendse, F.: Soil acidity and nutrient supply ratio as possible factors

617   determining changes in plant species diversity in grassland and heathland

618   communities, Biol. Conserv., 92, 151-161, https://doi.org/10.1016/S0006-3207

619   (99)00049-X, 2000.

620   Stevens, C. J., Thompson, K., Grime, J. P., Long, C. J., and Gowing, D. J.:

Contribution of acidification and eutrophication to declines in species richness of calcifuge grasslands along a gradient of atmospheric nitrogen deposition, Funct. Ecol., 24, 478-484, https://doi.org/10.1111/j.1365-2435.2009.01663.x, 2010.

Thomaes, A., De Keersmaeker, L., De Schrijver, A., Baeten, L., Vandekerkhove, K., Verstraeten, G., and Verheye, K.: Can soil acidity and light help to explain tree species effects on forest herb layer performance in post-agricultural forests?, Plant Soil, 373, 183-199, https://doi.org/10.1007/s11104-013-1786-x, 2013.

Tian, D. and Niu, S.: A global analysis of soil acidification caused by nitrogen addition, Environ. Res. Lett., 10, 024019, https://doi.org/10.1088/1748-9326/10/2/024019, 2015.

Tian, Q., Liu, N., Bai, W., Li, L., Chen. J., Reich, P. B., Yu Q., Guo, D., Smith, M. D., Knapp, A. K., Cheng, W., Lu, P., Gao, Y., Yang, A., Wang, T., Li, X, Wang, Z., Ma, Y., and Zhang, W.: A novel soil manganese mechanism drives plant species loss with increased nitrogen deposition in a temperate steppe, Ecology, 97, 65-74, https:// doi.org/10.1890/15-0917.1, 2016.

Tian, Q., Lu, P., Ma, P., Zhou, H., Yang, M., Zhai, X. Chen M., Wang, H., Li W., Bai, W., Lambers, H., and Zhang, W.: Processes at the soil-root interface determine the different responses of nutrient limitation and metal toxicity in forbs and grasses to nitrogen enrichment, J. Ecol., 109, 927-938, https://doi.org/10.1111/1365- 2745.13519, 2021.

Tian, Q., Lu, P., Zhai, X., Zhang, R., Zheng, Y., Wang, H., Nie, B., Bai, W., Niu, S., Shi, P., Yang, Y., Yang, D., Stevens, C., Lambers, H., and Zhang, W.: An integrated belowground trait‐based understanding of nitrogen‐driven plant diversity loss. Global Change Biol., 28, 3651-3664, https://doi.org/10.1111/ gcb.16147, 2022.

Tibbett, M., Gil-Martínez, M., Fraser, T., Green, I. D., Duddigan, S., De Oliveira, V. H., Raulund-Rasmussen, K., Sizmur, T. and Diaz, A.: Long-term acidification of pH neutral grasslands affects soil biodiversity, fertility and function in a heathland restoration, Catena, 180, 401-415, https://doi.org/10.1016/ j.catena.2019.03.013, 2019.

van Dobben, H. and de Vries, W.: Relation between forest vegetation, atmospheric deposition and site conditions at regional and European scales, Environ. Pollut., 158, 921-33, https://doi.org/10.1016/j.envpol.2009.09.015, 2010.

Violle, C., Navas, M. L., Vile, D., Kazakou, E., Fortunel, C., Hummel, I., and Garnier, E.: Let the concept of trait be functional!, Oikos, 116, 882-892, https://doi.org/10.1111/j.0030-1299.2007.15559.x, 2007.

Vitousek, P. M. and Howarth, R. W.: Nitrogen limitation on land and in the sea-how can it occur?, Biogeochemistry, 13, 87-115, https://doi.org/10.1007/BF00002772, 1991.

Wang, P., Guo, J., Xu, X., Yan, X., Zhang, K., Qiu, Y., Zhao, Q., Huang, K., Luo, X., Yang, F., Guo, H., and Hu, S.: Soil acidification alters root morphology, increases root biomass but reduces root decomposition in an alpine grassland, Environ. Pollut., 265, 115016, https://doi.org/10.1016/j.envpol.2020.115016, 2020.

Yang, F., Zhang, Z., Barberán, A., Yang, Y., Hu, S., Guo, H. Nitrogen-induced acidification plays a vital role driving ecosystem functions: Insights from a 6-year nitrogen enrichment experiment in a Tibetan alpine meadow, Soil Biol. Biochem., 153, 108107, https://doi.org/10.1016/j.soilbio.2020.108107, 2021.

Yang, G., Lü, X., Stevens, C. J., Zhang, G., Wang, H., Wang, Z., Zhang, Z., Liu, Z., and Han, X.: Mowing mitigates the negative impacts of N addition on plant species diversity, Oecologia, 189, 769-779, https://doi.org/10.1007/s00442-019-04353-9, 2019.

Yang, Y., Ji, C., Ma, W., Wang, S., Wang, S., Han, W., Mohammat, A., Robinson, D., and Smith, P.: Significant soil acidification across northern China's grasslands during 1980s-2000s, Global Change Biol., 18, 2292-2300, https://doi.org/10.1111/j.1365-2486.2012.02694.x, 2012.

Yu, H., He, N., Wang, Q., Zhu, J., Gao, Y., Zhang, Y., Jia, Y., and Yu, G.: Development of atmospheric acid deposition in China from the 1990s to the 2010s, Environ. Pollut., 231, 182-190, http://doi.org/10.1016/j.envpol.2017.08.014, 2017.

681   Yu, Q., Chen, Q., Elser, J. J., He, N., Wu, H., Zhang, G., Wu, J., Bai, Y., and Han, X.:

682   Linking stoichiometric homoeostasis with ecosystem structure, functioning and

683   stability, Ecol. Lett., 13, 1390-1399, https://doi.org/10.1111/j.1461-0248.

684   2010.01532.x, 2010.

685   Zhang, B., Cadotte, M. W., Chen, S., Tan, X., You, C., Ren, T., Chen, M., Wang, S.,

686   Li, W., Chu, C., Jiang, L., Bai, Y., Huang, J., and Han, X.: Plants alter their

687   vertical root distribution rather than biomass allocation in response to changing

688   precipitation, Ecology, 100, e02828, https://doi.org/10.1002 /ecy.2828, 2019.

689   Zhang, D., Peng, Y., Li, F., Yang, G., Wang, J., Yu, J., Zhou, G. and Yang, Y.: Above-

690   and belowground resource acquisition strategies determine plant species

691   responses to nitrogen enrichment. Ann. Bot., 128, 31-44, https://doi.org/10.1093

692   /aob/mcab032, 2021.

693   Zuchi, S., Cesco S., and Astolfi S.: High S supply improves Fe accumulation in

694   durum wheat plants grown under Fe limitation, Environ. Exp. Bot., 77, 25-32,

695   https://doi. org/10.1016/j.envexpbot.2011.11.001, 2012.

696

697

698

699

700

 Figures
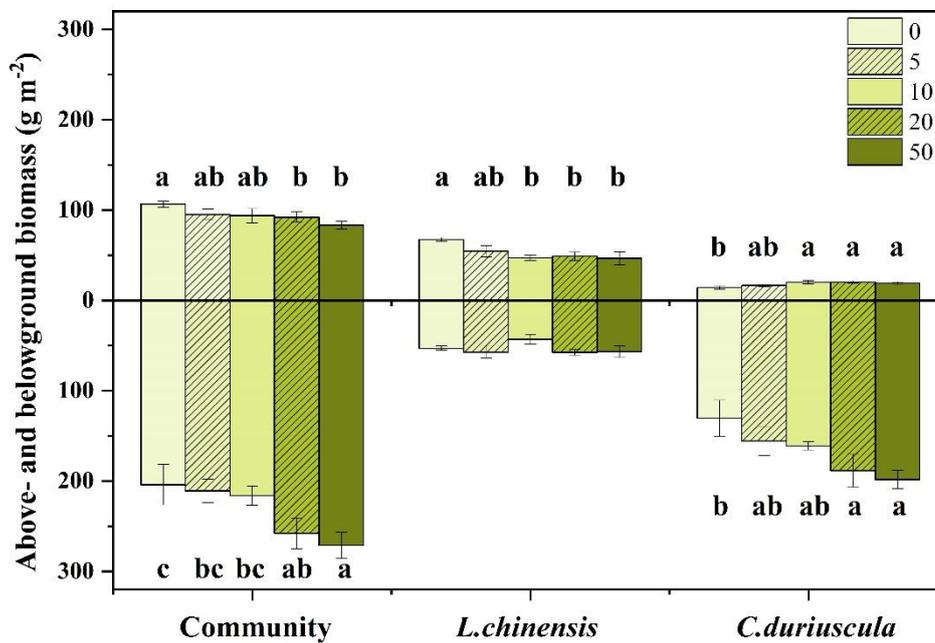
703 **Fig. 1** Effects of S addition on community and species aboveground and belowground

704 biomass. Bars are means ± the standard error. Lower case letters indicate significant

705 difference among treatments ($P < 0.05$).

706
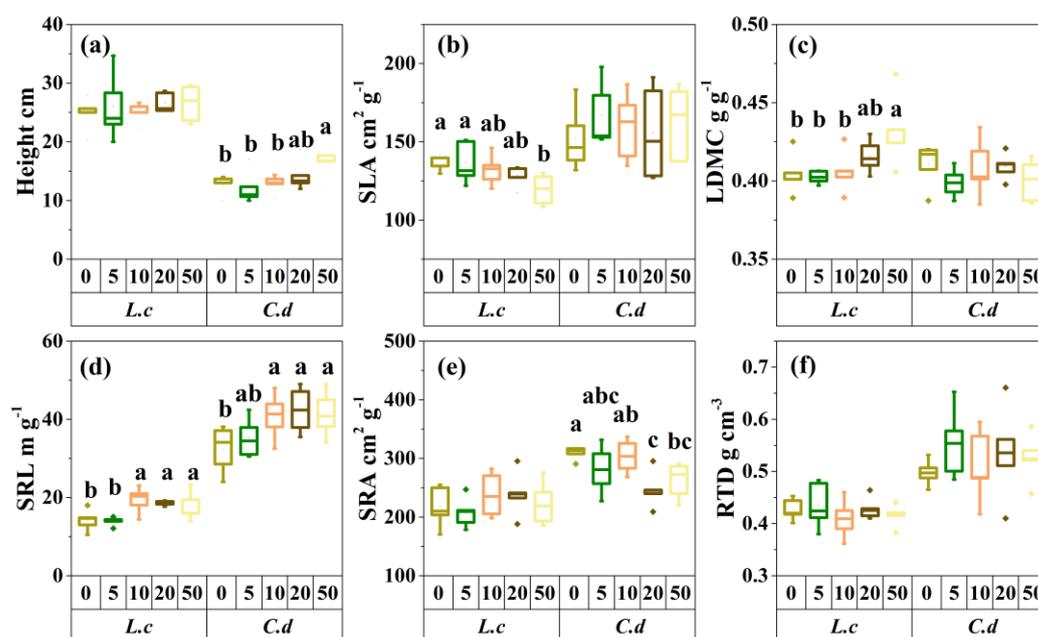
707

708 **Fig. 2** The response of the morphological traits to S addition for the two dominant
709 species in a meadow steppe. Abbreviations: SLA, Specific leaf area; LDMC, Leaf dry
710 matter content; SRL, specific root length; SRA, specific root area; RTD, root tissue
711 density; *L.c*, *L. chinensis*; *C.d*, *C. duriuscula*. Different letters above the bars indicate
712 significant influence among the S-addition level by one-way ANOVA at *P* < 0.05.

713
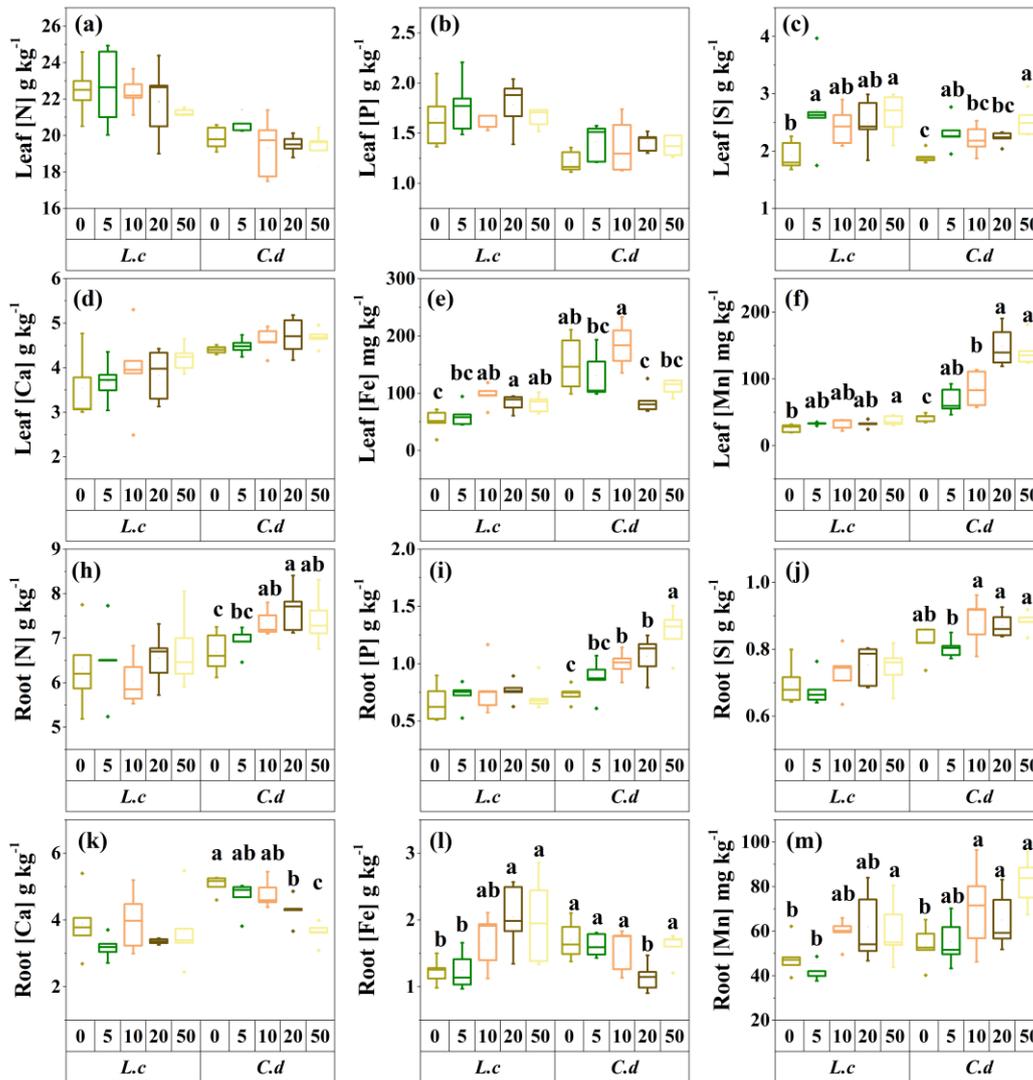
714

715 **Fig. 3** The response of the chemical traits to S addition for the two dominant species in
716 a meadow steppe. Abbreviations: Leaf [N], leaf N concentration; Leaf [P], leaf P
717 concentration; Leaf [S], leaf S concentration; Leaf [Ca], leaf Ca concentration; Leaf
718 [Fe], leaf Fe concentration; Leaf [Mn], leaf Mn concentration; Root [Ca], root Ca
719 concentration; Root [Fe], root Fe concentration; Root [Mn], root Mn concentration;

720 Root [N], root nitrogen concentration; Root [P], root phosphorus concentration; Root

721 [S], root sulfur concentration; *L.c*, *L. chinensis*; *C.d*, *C. duriuscula*. Different letters

722 above the bars indicate significant influence among the S-addition level by one-way

723 ANOVA at $P < 0.05$.

724

725

726

727

728
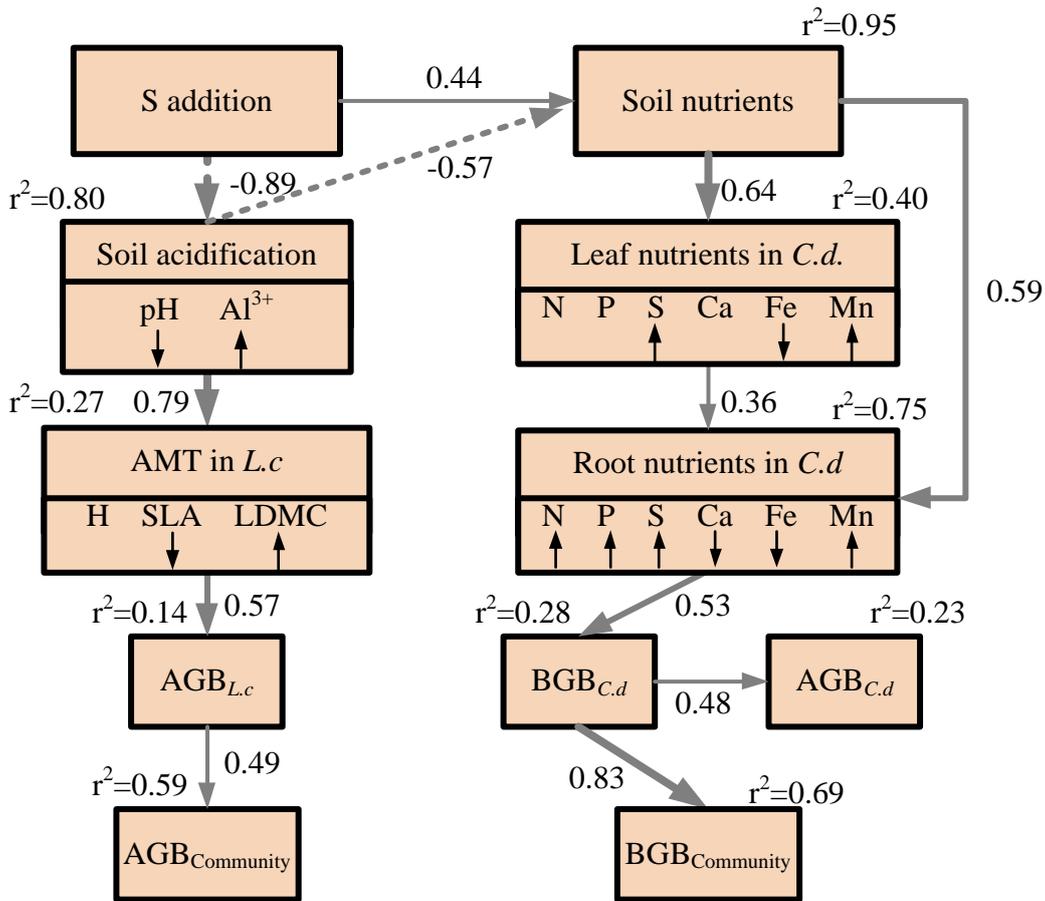
Fig. 4 Structural equation model of S addition on plant community biomass through the plausible pathways. Square boxes indicate the included variables in the analysis: S addition; Soil nutrients include soil NH_4^+-N and NO_3^--N concentrations, soil available phosphorus, soil available sulfur; soil exchangeable cations Ca^{2+}, Fe^{2+} and Mn^{2+}; soil acidification includes soil pH and exchangeable Al^{3+}; Aboveground morphological traits (AMT) includes plant height, specific leaf area, leaf dry matter content *in L. chinensis*; Leaf nutrients include leaf N, P, S, Ca, Fe, Mg concentrations in *C. duriuscula*; Root nutrients include root N, P, S, Ca, Fe, Mg concentrations in *C. duriuscula*; *C. duriuscula* aboveground biomass; *C. duriuscula* belowground biomass; *L. chinensis* aboveground biomass; Community aboveground biomass and belowground biomass. The symbols ↓ and ↑ indicate significant decrease or increase, respectively, with increasing S addition. The final SEM adequately fitted the data: $\chi^2 = 51.83$, DF = 40, $P = 0.10$, AIC = 103.83, n=25. R^2 values next to each response variable indicate the proportion of variation explained by relationships with other variables.

Solid and dashed arrows represent significant positive and negative pathways ($P < 0.05$),

respectively. Nonsignificant ($P > 0.05$) pathways are not shown. Values at each arrow

indicate the standard path coefficient, which is equivalent to the correlation coefficient.
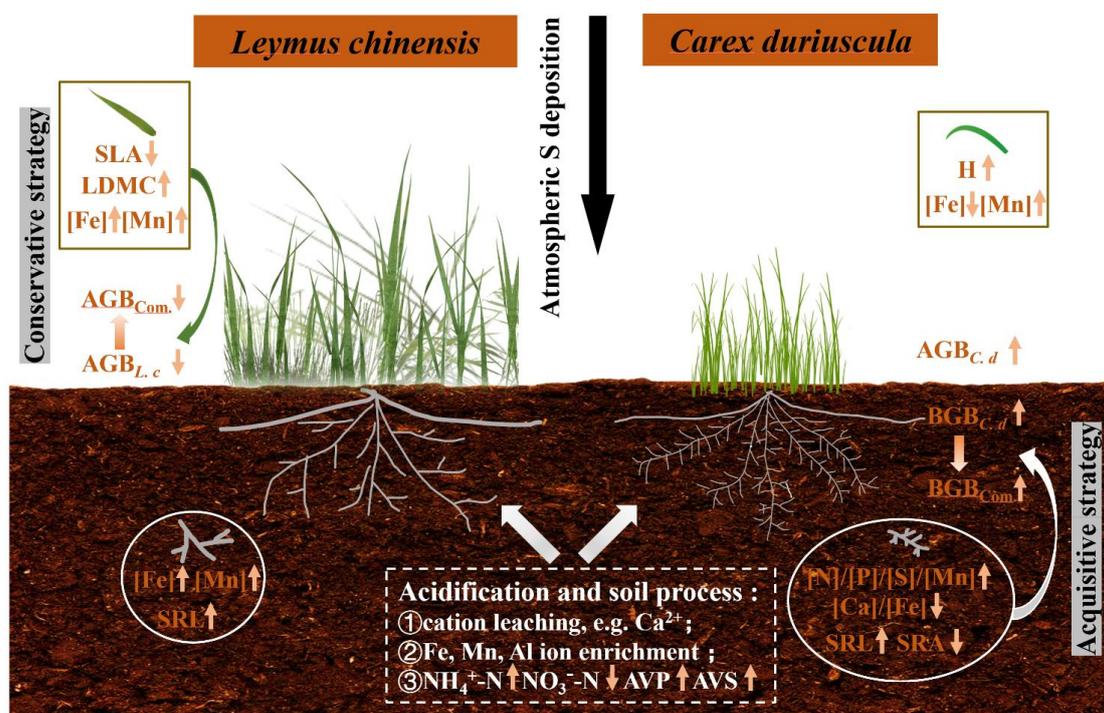
Fig. 5 Schematic diagram illustrating the ecological effects of S-induced soil

acidification on above- and belowground biomass and traits of two dominant species in

a meadow steppe. ↑ = increase in response to S addition; ↓ = decrease in response to S

addition; Com. = Community; AVP = Soil available phosphorus; AVS = Soil available

sulfur.

755 **Table**

756 **Table 1** Effects of S addition on soil abiotic variables. All numbers refer to the mean

757 (the standard error). Lower case letters indicate significant difference among treatments

758 ($P < 0.05$).

Soil parameters	S addition				
	0	5	10	20	50
Soil pH	6.95(0.06) a	6.70(0.07) ab	6.77(0.17) a	6.17(0.31) b	5.19 (0.20) c
Ex. Al^{3+}	5.49(0.72) b	5.49(0.18) b	6.84(0.45) b	9.09(1.44) b	20.07(3.24) a
Ammonium	4.76(0.31) b	4.36(0.08) b	4.92(0.68) b	4.67(0.22) b	8.33(1.73) a
Nitrate	4.88(0.42) a	5.44(0.73) a	5.45(1.01) a	4.60(0.95) a	1.41(0.31) b
AVP	5.20(0.64) b	5.27(0.71) b	4.58(0.35) b	6.94(0.60) a	7.08(0.38) a
AVS	8.78(0.78) c	10.30(1.33) c	15.09(1.89) c	40.64(8.56) b	114.41(6.85) a
DTPA-Fe	22.10(1.14) c	27.94(0.02) bc	30.62(0.02) bc	38.07(0.04) b	58.72(0.07) a
DTPA-Mn	19.26(1.56) c	27.43(1.43) bc	33.23(3.10) bc	41.66(4.40) b	79.60(7.54) a
Ex. Ca^{2+}	22.12(0.54) a	20.66(0.90) ab	20.14(1.09) ab	19.17(0.90) b	18.50(0.61) b

759 Note: Ex. Al^{3+}: Exchangeable Al^{3+}, mg kg^{-1}; Ammonium: soil NH_4^+-N concentration, mg kg^{-1};

760 Nitrate: soil NO_3^--N concentration, mg kg^{-1}; AVP: soil available phosphorus, mg kg^{-1}; AVS: soil

761 available sulfur, mg kg^{-1}; DTPA-Fe: Soil DTPA-Fe concentration, mg kg^{-1}; DTPA-Mn: Soil DTPA-

762 Mn concentration, mg kg^{-1}; Ex. Ca: Exchangeable Ca^{2+}, cmol kg^{-1}.

763